DE-FG05-80ET-53088-671 IFSR #671

Energetic Particle Drive for Toroidicity-Induced Alfvén Eigenmodes and Kinetic Toroidicity-Induced Alfvén Eigenmodes in a Low-Shear Tokamak

B.N. BREIZMAN[a)]
Institute for Fusion Studies
The University of Texas at Austin
Austin, Texas 78712
and
S.E. SHARAPOV[b)]
JET Joint Undertaking
Abingdon, Oxfordshire OX14 3EA, UK

October 1994
*****Revised*****

[a)] *Also at Budker Institute of Nuclear Physics, Novosibirsk 630090, Russia*
[b)] *Permanent address: Institute of Nuclear Fusion, Russian Research Centre "Kurchatov Institute," Kurchatov str. 46, Moscow 123182*

Energetic particle drive for toroidicity-induced Alfvén eigenmodes and kinetic toroidicity-induced Alfvén eigenmodes in a low-shear tokamak

B.N. Breizman[a)]

Institute for Fusion Studies, The University of Texas at Austin

Austin, Texas 78712

and

S.E. Sharapov[b)]

JET Joint Undertaking, Abingdon, Oxfordshire OX14 3EA, UK

Abstract

The structure of toroidicity-induced Alfvén eigenmodes (TAE) and kinetic TAE (KTAE) with large mode numbers is analyzed and the linear power transfer from energetic particles to these modes is calculated in the low shear limit when each mode is localized near a single gap within an interval whose total width $\Delta^{\rm out}$ is much smaller than the radius r_m of the mode location. Near its peak where most of the mode energy is concentrated, the mode has an inner scalelength $\Delta^{\rm in}$, which is much smaller than $\Delta^{\rm out}$. The scale $\Delta^{\rm in}$ is determined by toroidicity and kinetic effects, which eliminate the singularity of the potential at the resonant surface. This work examines the case when the drift orbit width of energetic particles Δ_b is much larger than the inner scalelength $\Delta^{\rm in}$, but arbitrary compared to the total width of the mode. It is shown that the particle-to-wave linear power transfer is comparable for the TAE and KTAE modes in this case. The ratio of the energetic particle contributions to the energetic particle drive for the TAE and KTAE modes is then roughly equal to the inverse ratio of the mode energies. It is found that, in the low shear limit the energetic particle drive for the KTAE modes can be larger than that for the TAE modes.

PACS Nos. : 52.35Bj, 52.35Qz, 52.55Fa, 51.10+y

[a)] Also at Budker Institute of Nuclear Physics, Novosibirsk 630090, Russia

[b)] Permanent address: Institute of Nuclear Fusion, Russian Research Centre "Kurchatov Institute," Kurchatov str. 46, Moscow 123182

I. INTRODUCTION

The problem of alpha particle confinement in a deuterium-tritium plasma has been long recognized to be an extremely important problem for achieving ignition in a tokamak reactor. For typical reactor parameters, the fusion-produced 3.5 MeV alpha particles comprise a considerable part of the total energy and have a highly-peaked radial profile.[1] Since these particles are super-Alfvénic, they are subject to enhanced transport that can result from the excitation of shear Alfvén modes or other magnetohydrodynamic (MHD) modes. Recent experiments[2,3] with neutral beam injection, have confirmed that Alfvén instabilities can indeed cause loss of energetic ions.

The purpose of the present work is to calculate the energetic particle drive for two types of weakly-damped Alfvén eigenmodes in a tokamak, namely, the toroidicity-induced Alfvén eigenmode (TAE)[4–7] and the kinetic TAE (KTAE).[8–10] The energetic particle drive for the TAE was initially calculated by Fu and Van Dam[11] in the zero orbit width approximation. Later, it was shown analytically[12] (and subsequently confirmed numerically[13]) that finite orbit width, even without finite Larmor radius (FLR) effects, can change the TAE growth rate from increasing linearly with toroidal mode number, to becoming independent of n, when the alpha particle radial excursion exceeds the inner layer spatial structure of the eigenfunction but is still small compared to the global ("outer") mode scale length. A more recent analysis[14] of the TAE and KTAE instabilities also has the restriction that the particle orbit width is small compared to the outer mode scale length.In this paper, we concentrate on the previously unexplored case in which the excursions of the alpha particles are comparable to or larger than the outer width of the excited mode. This situation is particularly relevant to the central region of an ignition plasma, where a large fraction of the alpha particles are concentrated. Their orbit widths can be comparable to the outer width of the mode even

for moderate values of the poloidal mode number, $m \approx 3 - 6$.

Our consideration will be restricted to the limit of low shear and large mode numbers, in which case each TAE or KTAE mode can be treated within a "single-gap" approximation. In addition, we assume that plasma pressure is negligibly small and that the tokamak has a large aspect ratio, for which the equilibrium magnetic field has circular flux surfaces.

We will employ a perturbation treatment, which requires the instability growth rate to be small compared to the characteristic frequency separation in the discrete mode spectrum and the mode structure to be insensitive to the relatively small number of energetic particles. The following comments need to be made about the validity and relevance of this approach.

First, the perturbation theory obviously breaks when the mode damping (not associated with the energetic particles) is so strong that it effects most of the mode structure. However, in this case, it is very difficult for a small number of fast particles to destabilize the mode. More likely, such nonperturbative modes will remain damped. Instability will preferentially occur for the weakly damped modes to which the perturbative treatment of the energetic particle drive is applicable. Hence, the perturbative approach is not just an assumption that we make to simplify the technical aspects of the problem but a natural way of treating the most interesting modes in the case when the number of fast particles is barely sufficient to drive the instability.

Second, the use of the perturbation theory for the calculation of the energetic particle drive does not necessarily mean that all the damping mechanisms can also be assessed this way. The subtlety is that part of the mode damping stems from tunneling or linear mode conversion, which is determined by the asymptotic wings of the mode eigenfunction, whereas the energetic particle drive is insensitive to these details. The fact that the drive and damping for the modes of interest are both small with no interdependence between them allows the damping mechanisms to be treated separately from the drive.

A detailed discussion of the mode damping and instability thresholds goes beyond the scope of this work. At this point we just refer to the papers that analyze various damping mechanisms, such as electron collisional damping,[9,15] radiative damping,[8] ion Landau damping,[16] and continuum damping.[6,7] For the weakly unstable modes, the total growth rate can then be written as a sum of the energetic particle driving term (which we calculate in this work) and the partial damping rates (calculated in the above mentioned references). The reason why we refrain here from discussing the instability thresholds is that the damping rates due to ion Landau damping, continuum damping and radiative damping can be exponentially sensitive to plasma parameters, which usually brings an inevitable uncertainty into quantitative estimates of the instability threshold, whereas the energetic particle drive is a fairly robust quantity.

In accordance with the perturbative approach we first determine the mode structure without any drive or damping and then calculate the energetic particle drive for this mode structure.

It should be noted that, in the large orbit width limit, the power transfer from the energetic particles to TAE and KTAE mode is independent of the inner structure of these modes. The instability growth rate can then be expressed as the ratio of the power transfer (which is insensitive to the inner mode structure) to the mode energy (which is mostly determined by the inner scale length). The power transfer turns out to be similar in magnitude for TAE and KTAE modes. Therefore, to compare TAE and KTAE growth rates, one should actually compare their mode energies expressed in terms of the inner scale lengths of the modes.

The rest of the paper is organized as follows. In Sec. II, we discuss the TAE/KTAE mode structure in the low-shear limit, which is particularly important in the center of a tokamak. Our method of the mode structure analysis is dfferent from that used in Refs. 9 and 10: we solve the problem directly in real space, rather than Fourier space, which should be physically more intuitive. In Sec. III, we use the obtained mode structure to calculate

the mode energy in terms of the amplitudes of the uncoupled asymptotic MHD solutions away from the gap. In Sec. IV, we find the linear power transfer to the TAE and KTAE modes from energetic particles. This section is based on the Lagrangian description of the wave-particle interaction, which is particularly convenient because it allows straightforward generalization to the nonlinear case.[17] In Sec. V, we discuss the particle orbit width effect of the instability growth rate and compare the growth rates for the TAE and KTAE modes. Finally, in Sec. VI, we briefly summarize the results of this work. Appendix A presents detailed calculations of the wave-particle coupling integral in the large-orbit limit.

II. TAE AND KTAE MODE STRUCTURE IN THE LOW SHEAR LIMIT

Both TAE and KTAE modes are known[4,9] to be associated with special magnetic surfaces ("gap" surfaces) at which the condition

$$q(r_m) = (m - 1/2)/n \ , \tag{1}$$

is satisfied, where m and n are the poloidal and toroidal mode numbers and $q(r)$ is the safety factor as a function of minor radius r. At the surface $r = r_m$, defined by Eq. (1), two cylindrical-geometry shear Alfvén modes with the poloidal mode numbers m and $m-1$ and the same toroidal mode number n are subject to strong poloidal coupling because they both satisfy the local dispersion equation $\omega = -k_{\|m}(r_m)v_A(r_m) = k_{\|m-1}(r_m)v_A(r_m)$, where $k_{\|m}(r) = [nq(r) - m]/Rq(r)$ is the parallel component of the wave vector, R being the major radius of the tokamak magnetic axis. For every poloidal harmonic m (here after n is fixed), there is also another surface $r = r_{m+1}$, defined by $q(r_{m+1}) = (m+1/2)/n$, where this harmonic is coupled to its upper sideband $(m+1)$. The distance between the surfaces r_m and r_{m+1} depends on the magnetic shear $S = rq'(r)/q(r)$ and can be estimated as

$$| \, r_{m+1} - r_m \, | \approx r_m/(nqS) \ . \tag{2}$$

At a sufficient distance from the gap surfaces, both the TAE and the KTAE can be described by the ideal MHD equations, which determine the so-called outer structure of the modes. In the high-m limit these MHD equations reduce to a single equation for each poloidal harmonic $\phi_m(r)$ of the wave electrostatic potential ϕ, expressed as

$$\phi(r,\vartheta,\varphi,t) = \exp[i(n\varphi - \omega t)] \sum_m \phi_m(r) \exp[-im\vartheta] + \text{c.c.} \tag{3}$$

Here (r,ϑ,φ) are the radial, poloidal, and toroidal coordinates. The resulting equation has the form[6]

$$L_m\phi_m \equiv \frac{d}{dr}\left(\frac{\omega^2}{v_A^2} - k_{\|m}^2\right)\frac{d\phi_m}{dr} - \frac{m^2}{r^2}\left(\frac{\omega^2}{v_A^2} - k_{\|m}^2\right)\phi_m = 0\ , \tag{4}$$

with the boundary condition $\phi_m(r) \to 0$ at $\mid r \mid \to \infty$. It follows from Eq. (4) that the outer width of the mode is

$$\Delta^{\text{out}} = r_m/m\ . \tag{5}$$

In the low-shear limit, Δ^{out} is much smaller than the distance between the gap surfaces defined by Eq. (2). Therefore, the coupling between different gaps is also small in this limit. Each eigenmode is then localized near its own gap surface, and there are only two poloidal harmonics (e.g., m and $m-1$ at $r = r_m$) that determine the mode structure.

To describe the mode structure near the gap surface, we must include toroidicity-induced coupling and nonideal effects in Eq. (4). The appropriately generalized set of equations for the two coupled poloidal harmonics has the form[9]:

$$L_m\phi_m + \varepsilon\frac{1}{4q^2R^2}\frac{d^2\phi_{m-1}}{dr^2} + \rho^2\frac{d^4\phi_m}{dr^4} = 0\ , \tag{6}$$

$$L_{m-1}\phi_{m-1} + \varepsilon\frac{1}{4q^2R^2}\frac{d^2\phi_m}{dr^2} + \rho^2\frac{d^4\phi_{m-1}}{dr^4} = 0\ , \tag{7}$$

with $\varepsilon = 5r_m/2R$ and the finite Larmor radius parameter ρ defined by

$$\rho^2 \equiv \frac{\rho_i^2}{4q^2R^2}\left\{\frac{3}{4} + \frac{T_e}{T_i}\right\}\ ,$$

where $\rho_i^2 = T_i/m_i\omega_{Bi}^2$; here T_e and T_i are the temperatures of the bulk electrons and ions respectively, and ω_{Bi} is the ion cyclotron frequency.

Toroidicity and nonideal effects are important only in the vicinity of the gap surface. These effects determine the inner scale of the mode, which is small compared to Δ^{out}. Nevertheless, most of the mode energy is concentrated in this inner region.

In the inner layer, Eqs. (6) and (7) can be integrated once to give a set of equations for the radial derivative quantities $U \equiv \frac{d\phi_m}{dz}$ and $V \equiv \frac{d\phi_{m-1}}{dz}$:

$$\lambda^2 \frac{d^2U}{dz^2} + (g+z)U + V = C_m, \tag{8}$$

$$\lambda^2 \frac{d^2V}{dz^2} + (g-z)V + U = -C_{m-1}, \tag{9}$$

where $z = 4\varepsilon^{-1}\left[nq(r) - m + 1/2\right]$ is a dimensionless radial variable, g is the frequency parameter defined by

$$g \equiv \frac{1}{\varepsilon}\left(\frac{4q^2R^2\omega^2}{v_A^2} - 1\right), \tag{10}$$

and λ is the normalized FLR parameter,

$$\lambda \equiv 4\frac{\rho_i}{r_m}\frac{mS}{\varepsilon^{3/2}}\left(\frac{3}{4} + \frac{T_e}{T_i}\right)^{1/2}.$$

By choosing parameter λ to be real we actually neglect the mode damping caused by the imaginary part of λ that is typically small compared to the real part.[9] It should be noted that the effect of Im λ on the mode structure is negligible since the singularity near the gap surface is already resolved by finite λ when λ is real. The mode damping rate associated with the imaginary part of λ can in fact be recovered from the dispersion relation obtained for real λ by means of analytical continuation. Namely, $\gamma_{\text{Im}\lambda} = \text{Im}\,\lambda\, d\omega/d\lambda$, where $\omega(\lambda)$ is the mode eigenfrequency for real λ. At small values of Im λ, this result agrees with the earlier calculations of the damping rate.[10]

In terms of the parameter g, the frequency gap corresponds to the interval $-1 < g < +1$, with $g = \pm 1$ being the upper and lower boundaries of the gap, respectively. The constants of

integration C_m and C_{m-1} in Eqs. (8) and (9) must be chosen so that the solution of Eqs. (8) and (9) matches onto the solution of Eq. (4).

We now examine the details of matching these two solutions. By expanding $k_{\|m}(r)$ about the gap surface in the low-shear limit, we rewrite Eq. (4) in the following form:

$$\frac{d}{dx}\, x\, \frac{d\phi_m}{dx} - x\, \frac{\phi_m}{S^2} = x\, \frac{d\phi_m}{dx}\ , \tag{11}$$

where $x = nq(r) - m + 1/2$. The term $x\,\frac{d\phi_m}{dx}$ on the right-hand side of this equation can be treated as a perturbation. Thus, to lowest order, we neglect this term and write the solution of Eq. (11) as

$$\phi_m^{\rm out} = -C_m K_0\left(\,|\,\frac{x}{S}\,|\,\right) = -C_m K_0\left(\,|\,\frac{r-r_m}{\Delta^{\rm out}}\,|\,\right)\ , \tag{12}$$

where $K_0(x)$ is the zeroth-order Macdonald function.[18] The integration constant C_m in Eq. (12) ensures that $d\phi_m/dr$ matches the asymptotic solution of Eqs. (8) and (9). It follows from Eq. (12) that, to lowest order in the shear, the outer solution is an even function of x. To find the odd parity corrections to ϕ_m and ϕ_{m-1}, we substitute Eq. (12) into the right-hand side of Eq. (11) and integrate Eq. (11) with the boundary conditions $\phi_m(-\infty) = \phi_m(+\infty) = 0$. We then find that ϕ_m has a discontinuity at small values of x:

$$J_m(S) \equiv \phi_m^{\rm out}\,|_{x\to -0} - \phi_m^{\rm out}\,|_{x\to +0} = C_m\,\frac{\pi^2 S}{4} + \mathcal{O}(e^{-1/S})\ . \tag{13}$$

A similar procedure applied to ϕ_{m-1} gives

$$J_{m-1}(S) \equiv \phi_{m-1}^{\rm out}\,|_{x\to -0} - \phi_{m-1}^{\rm out}\,|_{x\to +0} = -C_{m-1}\,\frac{\pi^2 S}{4} - \mathcal{O}(e^{-1/S})\ . \tag{14}$$

The jump conditions (13) and (14) are to be matched by the asymptotic solution of Eqs. (8) and (9). This requirement leads to dispersion relations for both the TAE and KTAE modes. We first reproduce the dispersion relation and the structure of the TAE mode, and then proceed to the kinetic TAE modes.

A. TAE mode

This mode exists for small λ, namely $\lambda < S^2$. Under somewhat stronger restriction, $\lambda \ll S^2$, Eqs. (8) and (9) become algebraic equations of the form

$$(g+z)U + V = C_m \ , \qquad (g-z)V + U = -C_{m-1} \ . \tag{15}$$

Note that, in the opposite limiting case ($\lambda \gg S^2$), this mode actually disappears because of the strong radiative damping. The solution of Eqs. (15) is

$$\phi_m^{\text{in}} = -\frac{gC_m + C_{m-1}}{(1-g^2)^{1/2}} \tan^{-1} \frac{z}{(1-g^2)^{1/2}} + \frac{C_m}{2} \ln \mid z^2 + (1-g^2) \mid + \text{const} \ , \tag{16}$$

$$\phi_{m-1}^{\text{in}} = \frac{gC_{m-1} + C_m}{(1-g^2)^{1/2}} \tan^{-1} \frac{z}{(1-g^2)^{1/2}} + \frac{C_{m-1}}{2} \ln \mid z^2 + (1-g^2) \mid + \text{const} \ . \tag{17}$$

The inner scale length of the TAE is therefore $z \sim (1-g^2)^{1/2}$ or, in dimensional form,

$$\Delta_{\text{TAE}}^{\text{in}} = \frac{\varepsilon}{4} \frac{r_m}{m} \frac{(1-g^2)^{1/2}}{S} \ . \tag{18}$$

Equations (16) and (17) give the following jumps of ϕ_m and ϕ_{m-1} at the inner layer:

$$\Delta \, \phi_m = -\pi \frac{gC_m + C_{m-1}}{(1-g^2)^{1/2}} \ , \tag{19}$$

$$\Delta \, \phi_{m-1} = \pi \frac{C_m + gC_{m-1}}{(1-g^2)^{1/2}} \ . \tag{20}$$

By matching Eqs. (19) and (20) and (13) and (14), we obtain

$$g \approx -1 + \frac{\pi^2 S^2}{8} \ , \qquad S \ll 1 \ , \tag{21}$$

and

$$C_m = C_{m-1} \ . \tag{22}$$

With the dispersion relation (21), Eq. (18) for the mode inner width takes the form

$$\Delta_{\text{TAE}}^{\text{in}} = \frac{\pi}{8} \frac{\varepsilon r_m}{m} \ll \Delta^{\text{out}} \ . \tag{23}$$

Finally, in the case of small shear, we note that the inner structure of the TAE mode is predominantly determined by the logarithmic part of the expressions in Eqs. (16) and (17).

B. Kinetic TAE modes

In contrast with the TAE mode whose eigenfrequency is located near the bottom of the gap (i.e., near $g \approx -1$) in the low shear limit, the spectrum of the KTAE modes tends to concentrate close to the top of the gap (i.e., near $g \approx 1$). In order to analyze the KTAE modes, we rewrite Eqs. (8) and (9) by introducing symmetric and antisymmetric combinations of U and V:

$$f \equiv \frac{U-V}{C_m + C_{m-1}} , \qquad F \equiv \frac{U+V}{C_{m-1} - C_m} . \tag{24}$$

Then we obtain the following equations:

$$\lambda^2 \frac{d^2F}{dz^2} + (g+1)F + \frac{zf}{\mu} = -1 , \tag{25}$$

$$\lambda^2 \frac{d^2f}{dz^2} + (g-1)f + \mu z F = 1 . \tag{26}$$

where $\mu = (C_{m-1} - C_m)/(C_m + C_{m-1})$.

Since g is close to unity, we need to retain the λ^2 term only in Eq. (26), whereas in Eq. (25) the term $\lambda^2 d^2F/dz^2$ can be dropped compared to $(g+1)F$. By neglecting this term we actually neglect the radiative damping of the KTAE modes. The modes will then appear to be real eigenmodes, whereas their life time is, in fact, finite because of the tunneling.[8] After the mode structure is found in the no-tunneling limit, the small damping due to tunneling can be calculated in a straightforward way.

With this simplification, Eqs. (25) and (26) reduce to a single equation for $f(z)$:

$$\lambda^2 \frac{d^2f}{dz^2} + (g-1)f - \frac{z^2}{2} f = 1 + \mu \frac{z}{2} . \tag{27}$$

We now find the solutions of Eq. (27) in two opposite limits, namely $\mu \to 0$ and $\mu \to \infty$. These solutions represent two independent polarizations of the KTAE modes. It can be proved that no value of μ other than $\mu \to 0$ or $\mu \to \infty$ is allowed in this problem; thereby the consistency of our approach can be justified.

We introduce the notation f^- for the $\mu \to \infty$ solution that satisfies the equation

$$\lambda^2 \frac{d^2 f^-}{dz^2} + (g-1) f^- - \frac{z^2}{2} f^- = \mu \frac{z}{2} , \tag{28}$$

with the constraint

$$\int dz \left(1 + \frac{z f^-}{\mu} \right) = -\frac{\pi^2 S}{2} , \tag{29}$$

which follows from the jump conditions (13) and (14). Note that f^- is obviously an odd function. Similarly, the $\mu \to 0$ solution is described by an even function f^+ that satisfies the equation

$$\lambda^2 \frac{d^2 f^+}{dz^2} + (g-1) f^+ - \frac{z^2}{2} f^+ = 1 , \tag{30}$$

with the constraint

$$\int dz f^+ = -\frac{\pi^2 S}{4} . \tag{31}$$

It follows from Eq. (28) that the characteristic width of f^- is of the order of $\lambda^{1/2}$. If we now estimate $f^- \approx \mu/\lambda^{1/2}$, then for $\lambda \ll S^2$ the left-hand side of Eq. (29) will formally be much smaller than the right-hand side. This indicates that the actual value of f^- is much larger than $\mu/\lambda^{1/2}$. To enhance f^- compared to this rough estimate, we must have the value of g be very close to an odd mode eigenvalue of the Schrödinger equation for a harmonic oscillator,

$$\lambda^2 \frac{d^2 f}{dz^2} + (g-1) f - \frac{z^2}{2} f = 0 , \tag{32}$$

i.e.,

$$g \approx 1 + \lambda(4p+3)/\sqrt{2} , \tag{33}$$

with $p = 0, 1, 2, \ldots$. Equation (28) will then provide a strongly resonant response to the "external force" $\mu z/2$, which will make f^- close to the p-th odd eigenfunction of Eq. (32),

$$f_p \equiv H_{2p+1}(\xi) \exp(-\xi^2/2) , \tag{34}$$

where H_{2p+1} is the Hermite polynomial, and $\xi = z(2\lambda^2)^{-1/4}$.

The appropriate solution of Eqs. (28) and (29) can be constructed perturbatively. Namely, we seek the solution of Eqs. (28) and (29) in the form

$$f^- = Af_p + \delta f \ , \tag{35}$$

$$g - 1 = \lambda(4p + 3 + \Delta^-)/\sqrt{2} \ , \tag{36}$$

where A is a constant, δf is much smaller than f_p, and Δ^- is a small correction to the eigenvalue given by Eq. (33). We substitute expressions (35) and (36) into Eq. (28), multiply the equation by f_p, and integrate over z to obtain

$$A = \frac{\mu}{2^{1/4}\lambda^{1/2}\Delta^-} \frac{\int \xi f_p d\xi}{\int f_p^2 d\xi} \ . \tag{37}$$

Finally, we use Eq. (29) to find

$$\Delta^- = -\frac{2^{5/4}\lambda^{1/2}}{\pi^2 S} \frac{(\int \xi f_p d\xi)^2}{\int f_p^2 d\xi} = -8\frac{2^{1/4}\lambda^{1/2}}{\pi^{3/2} S} \frac{(2p+1)!}{2^{2p}(p!)^2} \ . \tag{38}$$

We now turn to the solution of Eq. (30). Similar to f^-, the function f^+ is localized within the width $\Delta z = \lambda^{1/2}$. The magnitude of f^+ is of the order of $1/\lambda$. Since λ is a small parameter, this shows that the left-hand side of Eq. (31), which scales as $\lambda^{-1/2}$, is typically much larger than the right-hand side. One can then simplify Eq. (31) to

$$\int dz f^+ = 0 \ . \tag{39}$$

Same Eq. (30) with the constraint of Eq. (39) allows a straightforward analytical solution that can be obtained in Fourier representation which transforms Eq. (39) into the condition that the zeroth Fourier component of f^+ equals zero. The eigenvalues for this problem are equal to the odd eigenvalues given by Eq. (33) for the Schrödinger equation for an oscillator. The fact that the right-hand side of Eq. (31) is actually nonzero will only give a small correction to the eigenvalue g as determined by Eq. (33). This correction can be calculated perturbatively as follows. We seek the solution of Eqs. (30) and (31) in the form

$$f^+ = \frac{\sqrt{2}}{\lambda}(f_p^+ + \delta f) \ , \tag{40}$$

$$g - 1 = \lambda(4p + 3 + \Delta^+)/\sqrt{2} \tag{41}$$

with $| \delta f/f_p^+ | \ll 1$ and $| \Delta^+ | \ll 1$. The function f_p^+ is defined as the solution of the equation

$$\frac{d^2 f_p^+}{d\xi^2} + (4p+3) f_p^+ - \xi^2 f_p^+ = 1 \ , \tag{42}$$

where $\xi = z(2\lambda^2)^{-1/4}$. The explicit form of f_p^+ for the lowest eigenvalue ($p = 0$) is

$$f_{p=0}^+(\xi) = (1 - \xi \exp(-\xi^2/2) \int_0^\xi dx \exp(x^2/2)) \ . \tag{43}$$

For all other eigenvalues, f_p^+ can be constructed with the use of the recursion reation

$$f_{p+1}^+(\xi) = \frac{1}{4p+6} \left[1 + (\frac{d}{d\xi} - \xi)(\frac{d}{d\xi} - \xi) f_p^+ \right] \ , \tag{44}$$

which follows from Eqs. (62) and (63) of Sec. III. The validity of Eqs. (43) and (44) as well as the fact that f_p^+ satisfies Eq. (39) can be checked directly. We now substitute the expressions in Eqs. (40) and (41) into Eq. (30), multiply the equation by f_p^+, and integrate over z. By comparing the result with Eq. (31) we find that

$$\Delta^+ = \frac{\pi^2 S \lambda^{1/2}}{2^{11/4} \int d\xi (f_p^+)^2} = \frac{\pi^{1/2} S \lambda^{1/2}}{2^{3/4}} \frac{(2p+1)!}{2^{2p}(p!)^2} \ . \tag{45}$$

This formula includes the value of the integral $\int d\xi (f_p^+)^2$, which will be obtained later in Sec. III.

Thus, we conclude that, for very small values of λ, namely $\lambda \ll S^2$, the eigenvalues of both even and odd KTAE are close to the eigenvalues (33) for the odd eigenmodes of Eq. (32). This conclusion is consistent with the earlier observation of the eigenvalue pairing, made by Berk, Mett, and Lindberg.[10] Moreover, the eigenvalues for the even KTAE modes are close to (33) for any $\lambda \ll 1$. The situation is somewhat different for the odd KTAE modes: their eigenvalues remain close to these of Eq. (33) only as long as $\lambda \ll S^2$ [see Eq. (38)]. Equation (38) breaks down when λ exceeds S^2. At this point, the odd KTAE eigenvalues shift closer to the eigenvalues for the even states of the harmonic oscillator,

$$g - 1 = \lambda(4p + 1)/\sqrt{2} \ ,$$

where they remain as long as λ satisfies the condition $S^2 \ll \lambda \ll 1$. This result follows from the solution of Eq. (28), Fourier transformed, with the constraint

$$\int dz \left(1 + \frac{z f^-}{\mu}\right) = 0 \,. \tag{46}$$

This constraint is a simplification of Eq. (29) valid when $S^2 \ll \lambda \ll 1$.

In order to find the odd KTAE solution in the limit $S^2 \ll \lambda \ll 1$, we, following the analogy with the f^+-case, seek the solution of Eqs. (28) and (29) in the form

$$f^- = \frac{\mu}{2^{1/4}\lambda^{1/2}}(f_p^- + \delta f) \,, \qquad |\, \delta f / f_p^- \,| \ll 1 \,, \tag{47}$$

$$g - 1 = \lambda(4p + 1 + \tilde{\Delta}^-)/\sqrt{2} \,, \qquad |\, \tilde{\Delta}^- \,| \ll 1 \,, \tag{48}$$

where f_p^- is the solution of the equation

$$\frac{d^2 f_p^-}{d\xi^2} + (4p+1) f_p^- - \xi^2 f_p^- = \xi \,. \tag{49}$$

Then the correction $\tilde{\Delta}^-$ to the eigenvalue can be found to be

$$\tilde{\Delta}^- = \frac{\pi^2 S}{2^{5/4}\lambda^{1/2} \int (f_p^-)^2 d\xi} = \frac{\pi^{1/2} S}{2^{1/4}\lambda^{1/2}} \frac{(2p+1)!}{2^{2p}(p!)^2(2p+1)} \,. \tag{50}$$

The explicit expression for the integral $\int (f_p^-)^2 d\xi$ in this formula will be justified in Sec. III. To complete this section, we present the solution of Eq. (49) for the lowest eigenvalue ($p = 0$):

$$f_{p=0}^-(\xi) = -\exp(-\xi^2/2) \int_0^\xi dx \, \exp(x^2/2) \,. \tag{51}$$

III. MODE ENERGY

The energy of a radially localized toroidal Alfvén eigenmode can be written as

$$\delta W = \int d\varphi d\vartheta R r dr \frac{(\delta B_\vartheta)^2}{4\pi} \tag{52}$$

as long as $\delta B_\vartheta \gg \delta B_r$. This expression includes the perturbed plasma kinetic energy that is equal to the perturbed magnetic energy.

For TAE modes with the mode structure given by Eqs. (16) and (17), δW takes the form

$$\delta W = \frac{16\pi m R}{\varepsilon}\frac{c^2}{v_A^2}C_m^2 \ . \tag{53}$$

To calculate the wave energy for KTAE modes, we rewrite δW in terms of the quantities U and V as follows:

$$\delta W = \frac{8\pi m S R}{\varepsilon}\frac{c^2}{v_A^2}\int dz(\mid U \mid^2 + \mid V \mid^2) \ . \tag{54}$$

For the even KTAE-modes ($\mu \rightarrow 0$), the integrand reduces to

$$\mid U \mid^2 + \mid V \mid^2 \approx 2C_m^2 (f^+)^2 \ . \tag{55}$$

For the odd modes ($\mu \rightarrow \infty$), we have

$$\mid U \mid^2 + \mid V \mid^2 \approx 2C_m^2 \left(\frac{f^-}{\mu}\right)^2 \ . \tag{56}$$

We first calculate the energy of the odd KTAE modes for the case when $\lambda \ll S^2$, when f^- is given by Eqs. (35), (37), and (38) with f_p defined by Eq. (34). Then we obtain

$$\int_{-\infty}^{+\infty}\left(\frac{f^-}{\mu}\right)^2 d\xi = \frac{\pi^{7/2}S^2}{32\lambda^2}\frac{2^{2p}(p!)^2}{(2p+1)!} \ , \tag{57}$$

where table integrals of the Hermite polynomials have been used.[19] The final expression for the energy of these KTAE modes is

$$\delta W = \frac{\pi^{9/2} m S^3 R}{2^{3/4}\varepsilon\lambda^{3/2}}\frac{c^2}{v_A^2}F(p)C_m^2 \ , \tag{58}$$

where $F(p) = 2^{2p}(p!)^2/(2p+1)!$. At large values of p, the function $F(p)$ simplifies to the following asymptotic expression:

$$F(p) \approx \frac{1}{2}\sqrt{\frac{\pi}{p+1}} \ . \tag{59}$$

In order to find the dependence of the odd KTAE mode energy on the quantum number p in the limit $S^2 \ll \lambda \ll 1$, and also the dependence of the even mode energy on p for all $\lambda \ll 1$, we rewrite Eq. (42) in the form

$$S_+ S_- f_p^+ + 4(p+1)f_p^+ = 1 \ , \tag{60}$$

where $S_\pm = d/d\xi \pm \xi$. Similarly, Eq. (49) can be rewritten as

$$S_+ S_- f_p^- + (4p+2) f_p^- = \xi \, . \tag{61}$$

By applying the operator S_- to Eq. (60) and comparing the result with Eq. (61), we obtain

$$f_{p+1}^- = -S_- f_p^+ \, . \tag{62}$$

An analogous operation with Eq. (61) gives

$$(4p+2) f_p^+ = 1 - S_- f_p^- \, . \tag{63}$$

Two recursion relations can now be derived for the integrals of $(f_p^+)^2$ and $(f_p^-)^2$:

$$(4p+2) \int (f_p^+)^2 d\xi = \int (f_p^-)^2 d\xi \, , \tag{64}$$

$$4(p+1) \int (f_p^+)^2 d\xi = \int (f_{p+1}^-)^2 d\xi \, , \tag{65}$$

where

$$\int (f_0^-)^2 d\xi \equiv \int_{-\infty}^{+\infty} d\xi \, \exp(-\xi^2) (\int_0^\xi dz \, \exp(z^2/2))^2 = \frac{\pi^{3/2}}{2} \, .$$

Equations (64) and (65) show the following behavior of the odd mode energy with p:

$$\int (f_p^-)^2 d\xi / \int (f_0^-)^2 d\xi = \sqrt{\pi} \frac{\Gamma(p+1)}{\Gamma(p+1/2)} = \frac{2^{2p} (p!)^2 (2p+1)}{(2p+1)!} \, . \tag{66}$$

Note that, for large values of p, the energy increases as $\sqrt{\pi(p+1)}$. For the even mode, Eqs. (64) and (65) give

$$\int (f_p^+)^2 d\xi / \int (f_0^+)^2 d\xi = \sqrt{\pi} \frac{\Gamma(p+1)}{(2p+1)\Gamma(p+1/2)} = \frac{2^{2p} (p!)^2}{(2p+1)!} \, . \tag{67}$$

In contrast with the one for odd mode, this function asymptotically decreases with p. We finally include the obtained dependence on the quantum number p into the expressions for the energy of the odd and even KTAE modes, which gives

$$\delta W_{\text{odd}} = 8\pi^{5/2} \frac{mSRC_m^2}{2^{1/4} \varepsilon \lambda^{1/2}} \frac{c^2}{v_A^2} \frac{2^{2p} (p!)^2 (2p+1)}{(2p+1)!} \, , \qquad S^2 \ll \lambda \ll 1 \, , \tag{68}$$

$$\delta W_{\text{even}} = 8\pi^{5/2} \frac{2^{1/4} mSRC_m^2}{\varepsilon \lambda^{3/2}} \frac{c^2}{v_A^2} \frac{2^{2p} (p!)^2}{(2p+1)!} \, . \tag{69}$$

IV. PARTICLE-TO-WAVE POWER TRANSFER

In this section, we use the mode structure described in Sec. II in order to calculate the energetic particle contribution to the growth rate of Alfvén modes. Our derivation of the growth rate will be based on the wave-particle Lagrangian L that can be written as a sum of three terms:

$$L = L_w + L_p + L_{\rm int} \ . \tag{70}$$

Here, L_w is the wave Lagrangian for linear Alfvén modes, L_p is the energetic particle Lagrangian for their unperturbed motion in a tokamak, and $L_{\rm int}$ is the interaction term that depends on the dynamical variables of both waves and particles.

In the absence of nonideal effects, the Lagrangian for shear Alfvén waves has the following form:

$$L_w = \frac{c^2}{8\pi} \int dV \left[\frac{1}{v_A^2} \left(\nabla_\perp \frac{\partial \Phi}{\partial t} \right)^2 - \left(B_0 \nabla_\perp \frac{1}{B_0} (\mathbf{b}_0 \nabla) \Phi \right)^2 \right] \ , \tag{71}$$

where $\partial\Phi/\partial t = \phi$ is the electrostatic potential and $\mathbf{b}_0$ is the direction of the unperturbed magnetic field B_0.

We choose Φ to be a superposition of linear eigenmodes $\psi_n(\vartheta, \varphi, r)$ with eigenfrequencies ω_n:

$$\Phi = \sum_n A_n(t) \psi_n \exp(-i\omega_n t - i\alpha_n(t)) + \text{c.c.}, \tag{72}$$

where the mode amplitude $A_n(t)$ and the phase $\alpha_n(t)$ are assumed to be slowly varying functions of time. This representation reduces L_w to

$$L_w = \sum_n A_n^2 \frac{\partial \alpha_n}{\partial t} \frac{c^2 \omega_n}{2\pi} \int dV \frac{|\nabla_\perp \psi_n|^2}{v_A^2} \ . \tag{73}$$

It can be shown that this expression is also valid when nonideal effects are important near the gap surface; the function ψ_n should then be the eigenfunction with nonideal effects taken into account. This can be verified by generalizing the Lagrangian given by Eq. (71) in such a way that the modified Lagrangian gives Eqs. (6) and (7) for the linear modes.

To describe the motion of the energetic particles, we use the guiding center Lagrangian derived by Littlejohn.[20] For a large-aspect-ratio tokamak with circular flux surfaces, the unperturbed Lagrangian has the form[21]

$$L_p = \sum_{\text{particles}} \frac{e}{2c} B_0 r^2 \dot{\vartheta} + \dot{\varphi} \left(M u_\parallel (R + r\,\cos\vartheta) - \frac{e}{c} B_0 \int_0^r dr\, \frac{r}{q} \right)$$

$$- \tfrac{1}{2} M u_\parallel^2 - \mu B_0 \left(1 - \frac{r}{R} \cos\vartheta \right) , \tag{74}$$

where $\mu = M u_\perp^2 / 2B$ is the magnetic moment of the energetic particles. In this Lagrangian, the dynamical variables are: minor radius r, toroidal angle φ, poloidal angle ϑ, and parallel velocity $u_\parallel$. We restrict ourselves to a consideration of passing particles only, in which case $u_\parallel$ is nearly constant along the orbit. We also note that change in $u_\parallel$ due to the low frequency Alfvén perturbations is negligible. Thus, the toroidal motion of a passing particle can be described by

$$\varphi = \varphi_0 + u_\parallel t / R , \tag{75}$$

where φ_0 is the initial value of the toroidal angle φ.

With this simplification, φ and $u_\parallel$ become given quantities, rather than dynamical variables. The resulting reduced Lagrangian, which now describes the particle motion in the poloidal cross section, has the form

$$L_p = \frac{e}{c} B_0 \left(\frac{r^2}{2} \dot{\vartheta} + \left(u_\parallel^2 + \frac{\mu}{M} B_0 \right) \frac{r}{R \omega_B} \cos\vartheta - \frac{u_\parallel}{R} \int_0^r \frac{r}{q} dr \right) . \tag{76}$$

The interaction term in the Lagrangian (70) has been derived in Ref. 21. In the zero Larmor radius limit, we have

$$L_{\text{int}} = - \sum_{\text{particles}} e \left(\dot{\Phi} + u_\parallel (\mathbf{b}_0 \nabla) \Phi \right) . \tag{77}$$

We now simplify the particle Lagrangian L_p by changing independent variables from (r, ϑ) to $(\tilde{r}, \tilde{\vartheta})$, defined by

$$r = \tilde{r} + \Delta_b \cos\tilde{\vartheta} , \tag{78}$$

$$\vartheta = \tilde{\vartheta} - \frac{\Delta_b}{\tilde{r}} \sin\tilde{\vartheta} \ , \tag{79}$$

where $\tilde{r}$ is the mean radius of the particle orbit. The width of the particle orbit Δ_b is defined as

$$\Delta_b = \left(u_\parallel^2 + \frac{\mu}{M} B_0\right) \frac{q(\tilde{r})}{u_\parallel \omega_B} \tag{80}$$

and it is assumed that $\Delta_b \ll \tilde{r}$.

Transformations (78) and (79) change L_p to

$$L_p = \frac{e}{c} B_0 \left(\frac{\tilde{r}^2}{2}\dot{\tilde{\vartheta}} - \frac{u_\parallel}{R}\int_0^{\tilde{r}} \frac{r}{q} dr\right) \ . \tag{81}$$

The total Lagrangian for energetic particles and a single Alfvén mode can now be written as

$$L = \frac{eB_0}{c} \sum_{\text{particles}} \left(\frac{\tilde{r}^2}{2}\dot{\tilde{\vartheta}} - \int_0^{\tilde{r}} r\Omega dr\right) + \dot{\alpha} A^2 \frac{c^2 \omega_n}{2\pi} \int dV \frac{|\ \nabla_\perp \psi_n\ |^2}{v_A^2}$$

$$+ \sum_{\text{particles}} \text{Re} \sum_l A e^{-i\alpha} F_l e^{-i\tilde{\omega}t + in\varphi_0 + il\tilde{\vartheta}} \ , \tag{82}$$

with interaction amplitudes $F_l(\tilde{r})$ given by

$$F_l = \frac{ie}{\pi} \sum_m \int_0^{2\pi} \psi_{n,m}(\tilde{r} + \Delta_b \cos\tilde{\vartheta})(\tilde{\omega} + m\Omega) \exp\left(-im\tilde{\vartheta} + im\frac{\Delta_b}{\tilde{r}} \sin\tilde{\vartheta} - il\tilde{\vartheta}\right) d\tilde{\vartheta} \ , \tag{83}$$

where

$$\psi_{n,m}(r) \equiv \frac{1}{2\pi} \int_0^{2\pi} \psi_n(r, \vartheta, \varphi) \exp(im\vartheta - in\varphi) d\vartheta \ , \tag{84}$$

$\tilde{r}$ and $\tilde{\vartheta}$ are related to r and ϑ by Eqs. (78) and (79), and other notations are $\tilde{\omega} \equiv \omega_n - n u_\parallel / R$ and $\Omega \equiv u_\parallel / q(\tilde{r}) R$.

The Lagrangian given by Eq. (82) leads to the following set of equations for particle motion and wave dynamics:

$$\frac{eB_0}{c}\tilde{r}(\dot{\tilde{\vartheta}} - \Omega) + \text{Re} \sum_l A e^{-i\alpha} \frac{\partial F_l}{\partial \tilde{r}} e^{-i\tilde{\omega}t + in\varphi_0 + il\tilde{\vartheta}} = 0 \ , \tag{85}$$

$$\frac{eB_0}{c}\tilde{r}\dot{\tilde{r}} - \text{Re} \sum_l A e^{-i\alpha} il F_l e^{-i\tilde{\omega}t + in\varphi_0 + il\tilde{\vartheta}} = 0 \ , \tag{86}$$

$$\dot{A}\frac{c^2\omega_n}{\pi}\int dV\,\frac{|\,\nabla_\perp\psi_n\,|^2}{v_A^2}+\sum_{\text{particles}}\text{Re}\sum_l iF_l\exp(-i\alpha-i\tilde{\omega}t+in\varphi_0+il\tilde{\vartheta})=0\;, \qquad (87)$$

$$A\dot{\alpha}\frac{c^2\omega_n}{\pi}\int dV\frac{|\,\nabla_\perp\psi_n\,|^2}{v_A^2}+\sum_{\text{particles}}\text{Re}\sum_l F_l\exp(-i\alpha-i\tilde{\omega}t+in\varphi_0+il\tilde{\vartheta})=0\;. \qquad (88)$$

By linearizing Eqs. (85)–(88) and integrating them along the unperturbed particle orbits we obtain the following expression for the wave growth rate

$$\gamma\equiv\frac{\dot{A}}{A}=-\frac{\pi^2}{2ecB_0\omega_n}\left(\int dV\frac{|\,\nabla_\perp\psi_n\,|^2}{v_A^2}\right)^{-1}\sum_{\text{particles}}\sum_l\frac{l}{\tilde{r}}\frac{\partial}{\partial\tilde{r}}\left[|\,F_l\,|^2\,\delta(\tilde{\omega}-l\Omega)\right]\;. \qquad (89)$$

By its definition, the growth rate can also be written as half the ratio of the particle-to-wave power transfer P to the wave energy δW:

$$\gamma=\frac{P}{2\delta W}\;, \qquad (90)$$

where

$$\delta W\equiv\frac{A^2c^2{\omega_n}^2}{2\pi}\int dV\frac{|\,\nabla_\perp\psi_n\,|^2}{v_A^2}\;. \qquad (91)$$

By combining Eqs. (89)–(91) we find

$$P=-\frac{\pi c\omega_n A^2}{2eB_0}\sum_{\text{particles}}\sum_l\frac{l}{\tilde{r}}\frac{\partial}{\partial\tilde{r}}\left[|\,F_l\,|^2\,\delta(\tilde{\omega}-l\Omega)\right]\;. \qquad (92)$$

In contrast to the wave energy, which is mostly determined by the inner scale length of the mode, the power transfer is insensitive to the mode inner structure. This conclusion requires only that the particle orbit width Δ_b be greater than the inner scale length of the mode.[12] Therefore, it is allowable to formally replace the exact eigenfunction ψ_n in the interaction amplitude with the asymptotic expression for ψ_n that describes the outer mode structure. Despite the logarithmic singularity in the outer solution (12), the integral for F_l converges due to the finite particle orbit width.

Since F_l enters γ and P as a coefficient in front of the δ-function, we only need to calculate F_l for $\tilde{\omega}=l\Omega$. We also take into account that, in the low shear limit, each eigenmode has

only two components (m and $m-1$), with $\psi_{n,m}$ and $\psi_{n,m-1}$ given by

$$\psi_{n,m} = -\frac{iC_m}{A\omega_n} e^{i\alpha} K_0 \left(\mid \frac{r - r_m}{\Delta^{\text{out}}} \mid \right) , \tag{93}$$

$$\psi_{n,m-1} = \pm \psi_{n,m} \tag{94}$$

where the plus sign in Eq. (94) refers to the TAE and even KTAE modes, and the minus sign refers to the odd KTAE modes. Equation (83) with the mode structure of Eqs. (93) and (94) gives

$$F_l = \frac{e\Omega C_m}{\pi \omega_n A} e^{i\alpha} \int_0^{2\pi} \left((m+l) \pm (m+l-1) e^{i\tilde{\vartheta}} \right) K_0 \left(\mid \frac{\tilde{r} + \Delta_b \cos\tilde{\vartheta} - r_m}{\Delta^{\text{out}}} \mid \right)$$
$$\times \exp\left(-im\tilde{\vartheta} + im\frac{\Delta_b}{\tilde{r}} \sin\tilde{\vartheta} - il\tilde{\vartheta} \right) d\tilde{\vartheta} . \tag{95}$$

We now substitute F_l into Eq. (92) for the power transfer and note that the sum over the energetic particles can be changed to an integral over the phase volume with the unperturbed particle distribution f. After integration by parts over $\tilde{r}$, we obtain

$$P = \frac{2\pi^3 c \omega_n R A^2}{eB_0} \int d\tilde{r} \int d^3v \sum_l l \frac{\partial f}{\partial \tilde{r}} \mid F_l \mid^2 \delta(\tilde{\omega} - l\Omega) . \tag{96}$$

After the δ-function is eliminated by the velocity space integration, the integrand, except for F_l, becomes a smooth function of $\tilde{r}$, with the spatial scale length determined by the distribution of energetic particles. The function F_l, unlike other terms, is localized within a much narrower interval, which is determined by the particle orbit width and the outer mode width. Hence, the $\tilde{r}$ integral only involves F_l, while all other functions of $\tilde{r}$ in Eq. (96) can be evaluated at the mode location. With this approximation we find

$$P = \frac{2\pi e c R \Delta^{\text{out}} C_m^2}{\omega_n B_0} \int d^3v \Omega^2 \frac{\partial f}{\partial r} \sum_s (s-m) I \delta\left(\tilde{\omega} + (m-s)\Omega\right) , \tag{97}$$

where the coupling integral I is defined as

$$I\left(s, \frac{\Delta_b}{\Delta^{\text{out}}}\right) \equiv \int_0^{2\pi} d\vartheta \int_0^{2\pi} d\tilde{\vartheta} (s \pm (s-1)e^{i\tilde{\vartheta}})(s \pm (s-1)e^{-i\vartheta})$$

$$\times \exp\left(i\frac{\Delta_b}{\Delta^{\rm out}}\left(\sin\tilde{\vartheta}-\sin\vartheta\right)-is(\tilde{\vartheta}-\vartheta)\right)$$

$$\times \int dr K_0\left(\mid r \mid\right) K_0\left(\mid r+\frac{\Delta_b}{\Delta^{\rm out}}\left(\cos\tilde{\vartheta}-\cos\vartheta\right)\mid\right) . \qquad (98)$$

For small values of $\Delta_b/\Delta^{\rm out}$, this integral has been calculated in Ref. 12. For large values of $\Delta_b/\Delta^{\rm out}$, it is calculated in Appendix A of the present work. The results of both calculations can be summarized as follows:

$$I\left(s,D\right)=4\pi^2\frac{1}{D}(s^2+(s-1)^2)\ , \qquad D\gg\sqrt{s^2+(s-1)^2}\ , \qquad (99)$$

$$I\left(s,D\right)=16\pi^2 D\left(\frac{s^2}{4s^2-1}+\frac{(s-1)^2}{4(s-1)^2-1}\right)\ , \qquad D\ll\sqrt{s^2+(s-1)^2}\ . \qquad (100)$$

V. LARGE ORBIT EFFECT ON THE MODE GROWTH RATE

In this section, we use the term "large orbit" as opposed to the term "finite orbit" of Ref. 12 in order to emphasize that the orbit width can now be arbitrary (not necessarily small) compared to the outer width of the mode. Of particular interest is the case in which these two quantities are comparable to each other. Note that the inner scale length of the mode is then negligibly small compared to the orbit width. Our conclusion here will be that the large orbit effects make the energetic particle drive a decreasing function of the mode number for both the TAE and the KTAE modes, when the mode number is sufficiently large.

We will evaluate the drive for a slowing-down distribution function of the energetic ions, taken in the form

$$f=\frac{3\beta_\alpha B^2}{16\pi^2 M_\alpha v_0^2}\frac{\Theta(v_0-v)}{v^3}h(\kappa)\ , \qquad (101)$$

where $\Theta(x)$ is the step function, v_0 is the injection velocity of energetic ions, and $h(\kappa)$ with $\kappa\equiv v_\parallel/v$ is the pitch-angle distribution. We choose

$$h(\kappa)=\frac{\cosh(\kappa/\kappa_0)}{\kappa_0\sinh(1/\kappa_0)}\ , \qquad (102)$$

where κ_0 is the anisotropy parameter. For an isotropic distribution we have $\kappa_0 \gg 1$, so that $h = 1$. The distribution function in Eq. (101) is normalized to the average beta of the energetic ions, i.e.,

$$\beta_\alpha = (8\pi M_\alpha/3B^2) \int d^3v v^2 f \ . \tag{103}$$

We first calculate the power transfer P in Eq. (97) for a strongly anisotropic beam-like distribution with $\kappa_0 \ll 1$ assuming that $v_0 > v_A$. In this case, the major contribuion to P comes from the principal resonances ($s = 0$ and $s = 1$). In Fig. 1a we show the numerically evaluated coupling integral $I(D) \equiv I(0, D) = I(1, D)$ for these resonances. Shown by the dashed line in the same figure is the function $I(D)$ given by the asymptotic formulas (99) and (100). Except for intermediate values of D, these formulas show a reasonably good agreement with the numerical results. The velocity integration in Eq. (97) eliminates the delta function and gives

$$P = -3\frac{v_A^2}{v_0^2}\frac{c^2\beta'_\alpha}{\omega_n}C_m^2\frac{I(D)}{D} \ , \tag{104}$$

where $D = (qmv_A)/(r_m\omega_B)$ and the function $I(D)/D$ is shown in Fig. 1b. We now find from Eqs. (104), (90) and (53) that the contribution of the energetic ions to the growth rate of the TAE mode is

$$\frac{\gamma_{\rm TAE}}{\omega_{\rm TAE}} = -\frac{15}{16\pi}r_m\beta'_\alpha q^2\frac{v_A^2}{v_0^2}\frac{I(D)}{D} \ , \tag{105}$$

where $D = (qmv_A)/(r_m\omega_B)$. In accordance with the result obtained in Ref. 12 for moderate values of m, this growth rate is relatively insensitive to the mode number m as long as the outer mode width r_m/m exceeds the particle orbit width. For larger values of m, the growth rate decreases with increasing m due to the orbit width effect. Using the fact that the principal resonance terms in the particle-to-wave power transfer are identical for the TAE and KTAE modes, we can write the odd KTAE growth rate as follows:

$$\frac{\gamma_{\rm KTAE}}{\omega_{\rm KTAE}} = -\frac{30}{\pi^{9/2}2^{1/4}}r_m\beta'_\alpha q^2\frac{v_A^2}{v_0^2}\frac{I(D)}{D}\frac{(2p+1)!}{2^{2p}(p!)^2}\left(\frac{\lambda}{S^2}\right)^{3/2} \ , \qquad \lambda \ll S^2 \ , \tag{106}$$

$$\frac{\gamma_{\rm KTAE}}{\omega_{\rm KTAE}} = -\frac{15}{8}\frac{2^{1/4}}{\pi^{5/2}} r_m \beta'_\alpha q^2 \frac{v_A^2}{v_0^2}\frac{I(D)}{D}\frac{(2p+1)!}{2^{2p}(p!)^2(2p+1)}\left(\frac{\lambda}{S^2}\right)^{1/2}, \qquad S^2 \ll \lambda \ll 1\,. \tag{107}$$

The second of these two equations shows that the growth rate for the KTAE mode can be greater than that for the TAE mode, when the condition $S^2 \ll \lambda \ll 1$ is satisfied. Moreover, under the same condition, the TAE mode has a much stronger radiative damping than that for the KTAE mode. This condition obviously requires that the shear be small. Otherwise, the KTAE mode appears to be less unstable than the TAE mode, in agreement with the results of Ref. 14.

We finally present the expression for the power transfer for the case in which the distribution function is isotropic. Similarly to Eq. (104), we retain only the principal resonances and use Fig. 1 for the coupling integral. We then obtain

$$P = -m\frac{v_A^2}{v_0^2}\frac{c^2\beta'_\alpha}{\omega_n} C_m^2 \frac{3}{2}\int_{v_A}^{v_0} dv \frac{v_A^2+v^2}{v^2 v_A}\frac{I(D)}{D}\,, \tag{108}$$

where

$$D = \frac{qm(v_A^2+v^2)}{2v_A r_m \omega_B}\,.$$

For moderate mode numbers, this expression reproduces the corresponding result obtained in Ref. 12. For large mode numbers, Eq. (108) shows that the drive decreases due to the orbit width effect regardless of whether it is TAE or KTAE mode.

VI. SUMMARY

In conclusion, we have obtained the eigenfunctions and the eigenvalues of the TAE and KTAE modes in the low-shear limit by solving the mode equations in real space. Within this approach, the initial mode equation splits into two separate equations: one for the even parity modes and one for the odd parity modes, which allows us to relate the spectrum of the KTAE modes to the spectrum of a harmonic quantum oscillator. We have also calculated the energetic particle drive for both the TAE and the KTAE modes without restrictions on

the ratio of the particle drift orbit width to the "outer" mode width. We note that the particle-to-wave power transfer is insensitive to the "inner" width of the mode, as long as the particle orbit width is greater than the mode inner scale length. Our analysis shows that a) the inner width of the odd KTAE modes and the energetic particle drive for these modes are typically larger than those for the even KTAE modes; and b) for large mode numbers, the energetic particle drive for all modes decreases due to the orbit width effect. A distinctive feature of the low shear case is that it allows the KTAE modes to be more unstable than the TAE mode.

Acknowledgments

We are grateful to H. L. Berk, J. W. Van Dam, and M. S. Pekker for important discussions. This work was supported by the U.S. Department of Energy, Contract No. DE-FG05-80ET-53088.

Appendix A: Coupling Integral

The general form of the coupling integral given by Eq. (98) is

$$I(s,D) = \int_0^{2\pi} d\vartheta \int_0^{2\pi} d\tilde{\vartheta}[s \pm (s-1)e^{i\tilde{\vartheta}}][s \pm (s-1)e^{-i\vartheta}]$$
$$\times \exp\left(iD\left(\sin\tilde{\vartheta} - \sin\vartheta\right) - is(\tilde{\vartheta} - \vartheta)\right)$$
$$\times \int dr K_0\left(\mid r \mid\right) K_0\left(\mid r + D\left(\cos\tilde{\vartheta} - \cos\vartheta\right) \mid\right) . \qquad \text{(A1)}$$

For large values of D, the principal contribution to this integral comes from the integration region near the line $\vartheta \approx \tilde{\vartheta}$, so that we have approximately

$$I = \int_0^{2\pi} d\vartheta \left[s^2 + (s-1)^2 \pm 2s(s-1)\,\cos\vartheta\right] \int d(\tilde{\vartheta} - \vartheta) \exp\left(i(\tilde{\vartheta} - \vartheta)D\,\cos\vartheta\right)$$
$$\times \int dr K_0\left(\mid r \mid\right) K_0\left(\mid r - (\tilde{\vartheta} - \vartheta)D\,\sin\vartheta \mid\right) . \qquad \text{(A2)}$$

By changing the integration variable from $(\tilde{\vartheta} - \vartheta)$ to $x = (\tilde{\vartheta} - \vartheta)D$, we obtain

$$I = \frac{1}{D}\int_0^{2\pi} d\vartheta \left[s^2 + (s-1)^2 \pm 2s(s-1)\,\cos\vartheta\right] \int dx \cos\left(x\,\cos\vartheta\right)$$
$$\times \int dr K_0\left(\mid r \mid\right) K_0\left(\mid r - x\,\sin\vartheta \mid\right) . \qquad \text{(A3)}$$

The term with the $\pm$ sign does not contribute to this integral because $\cos\vartheta$ changes its sign when the integration variable changes from ϑ to $\pi - \vartheta$, whereas other terms of the integrand remain unchanged. Therefore,

$$I = \frac{2}{D}\left(s^2 + (s-1)^2\right) \int_0^{\pi} d\vartheta \int dx \cos\left(x\,\cos\vartheta\right) \int dr K_0\left(\mid r \mid\right) K_0\left(\mid r - x\,\sin\vartheta \mid\right) . \qquad \text{(A4)}$$

Here, we have used the symmetry features of the integrand in order to present I as twice the integral over ϑ from 0 to π. We now introduce a new integration variable y in place of of x:

$$y = x\,\sin\vartheta - r\ . \qquad \text{(A5)}$$

Then Eq. (A4) takes the form

$$I = \frac{2}{D}\left(s^2 + (s-1)^2\right) \int_0^\pi d\vartheta \frac{1}{\sin\vartheta} \left(\int dy \cos\left(y \frac{\cos\vartheta}{\sin\vartheta} \right) K_0\left(|\, y \,|\right) \right)^2 . \tag{A6}$$

Integration over y gives

$$I = \frac{2\pi^2}{D}\left(s^2 + (s-1)^2\right) \int_0^\pi d\vartheta \, \sin\vartheta \, . \tag{A7}$$

Finally, we obtain

$$I = \frac{4\pi^2}{D}\left(s^2 + (s-1)^2\right) \, . \tag{A8}$$

REFERENCES

[1] K. Tomabechi, J. R. Gilleland, Yu. A. Sokolov, R. Toschi, and ITER Team, Nucl. Fusion **31**, 1135 (1991).

[2] K. L. Wong, R. J. Fonck, S. F. Paul, D. R. Roberts, E. D. Fredrickson, R. Nazikian, H.K. Park, H. Bell, N. L. Bretz, R. Budny, S. Cohen, G. W. Hammett, F. C. Jobes, D. M. Meade, S. S. Medley, D. Mueller, Y. Nagayama, D. K. Owens, and E. J. Synakowski, Phys. Rev. Lett. **66**, 1874 (1991).

[3] W. W. Heidbrink, E. J. Strait, E. Doyle, G. Sager and R. Snider, Nucl. Fusion **31**, 1635 (1991).

[4] C. Z. Cheng, Liu Chen and M. S. Chance, Ann. Phys. **161**, 21 (1985).

[5] C. Z. Cheng and M. S. Chance, Phys. Fluids **29**, 3695 (1986).

[6] M. N. Rosenbluth, H. L. Berk, J. W. Van Dam, and D. M. Lindberg, Phys. Rev. Lett. **68**, 596 (1992).

[7] F. Zonca and L. Chen, Phys. Rev. Lett. **68**, 592 (1992).

[8] R. R. Mett and S. M. Mahajan, Phys. Fluids B **4**, 2885 (1992).

[9] J. Candy and M. N. Rosenbluth, Physics of Plasmas **1**, 356 (1994)

[10] H. L. Berk, R. R. Mett, and D. M. Lindberg, Phys. Fluids B **5**, 3969 (1993).

[11] G. Y. Fu and J. W. Van Dam, Phys. Fluids B **1**, 1949 (1989).

[12] H. L. Berk, B. N. Breizman, and H. Ye, Phys. Lett A **162**, 475 (1992).

[13] G. Y. Fu and C. Z. Cheng, Phys. Fluids B 4, 3722 (1992).

[14] J. Candy and M. N. Rosenbluth, Plasma Physics and Controlled Fusion **35**, 957 (1993).

[15] N. N. Gorelenkov and S. E. Sharapov, Physica Scripta **45**, 163 (1992).

[16] R. Betti and J. P. Freidberg, Phys. Fluids B **4**, 1465 (1992).

[17] H. L. Berk, B. N. Breizman, S. M. Mahajan, M. S. Pekker, J. W. Van Dam, H. V. Wong, D. Borba, S. E. Sharapov, J. Candy, M. S. Chu, R. R. Mett, and M. N. Rosenbluth, in *Proceedings of the 15th International Conference on Plasma Physics and Controlled Nuclear Fusion Research, 1994*, Seville (International Atomic Energy Agency, Vienna, 1995).

[18] M. Abramowitz and I. A. Stegun, eds., *Handbook of Mathematical Functions with Formulas, Graphs and Mathematical Tables* (National Bureau of Standards Applied Mathematics Series 55, Washington, D.C., 1964).

[19] I. S. Gradshteyn and I. M. Ryzhik, *Table of Integrals, Series, and Products* (Academic Press, New York, London, 1980).

[20] R. G. Littlejohn, J. Plasma Phys. **29** 111 (1983).

[21] H. L. Berk, B. N. Breizman, and H. Ye, Phys. Fluids B **5**, 1506 (1993).

FIGURE CAPTIONS

Fig. 1. Coupling integral $I(D)$ for the principal resonances ($s = 0; 1$):

a) asymptotic expression (dashed line) and numerical results for $I(D)$ (solid line);

b) function $I(D)/D$ used in Eqs. (104), (105), and (108).

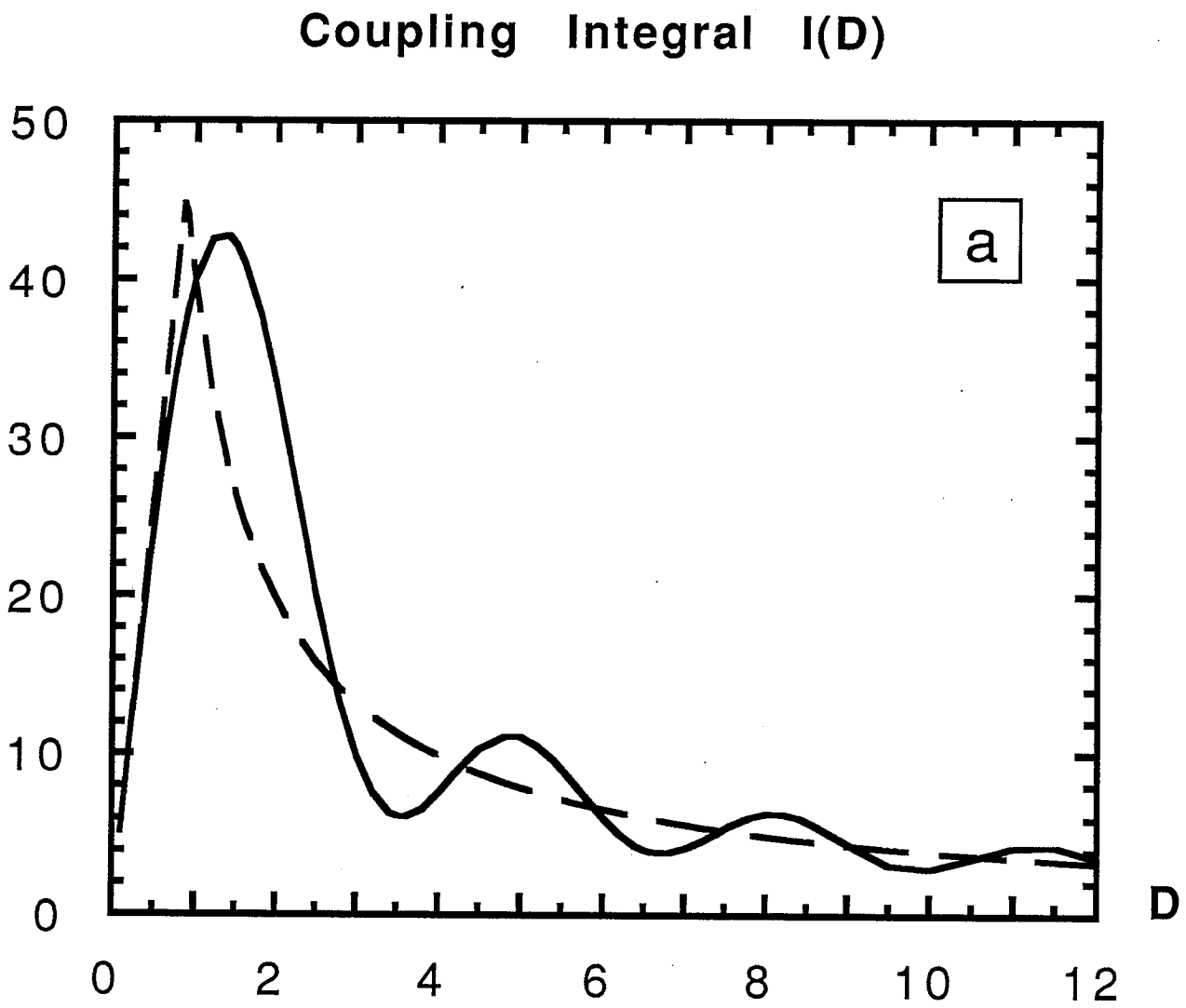

Fig. 1a

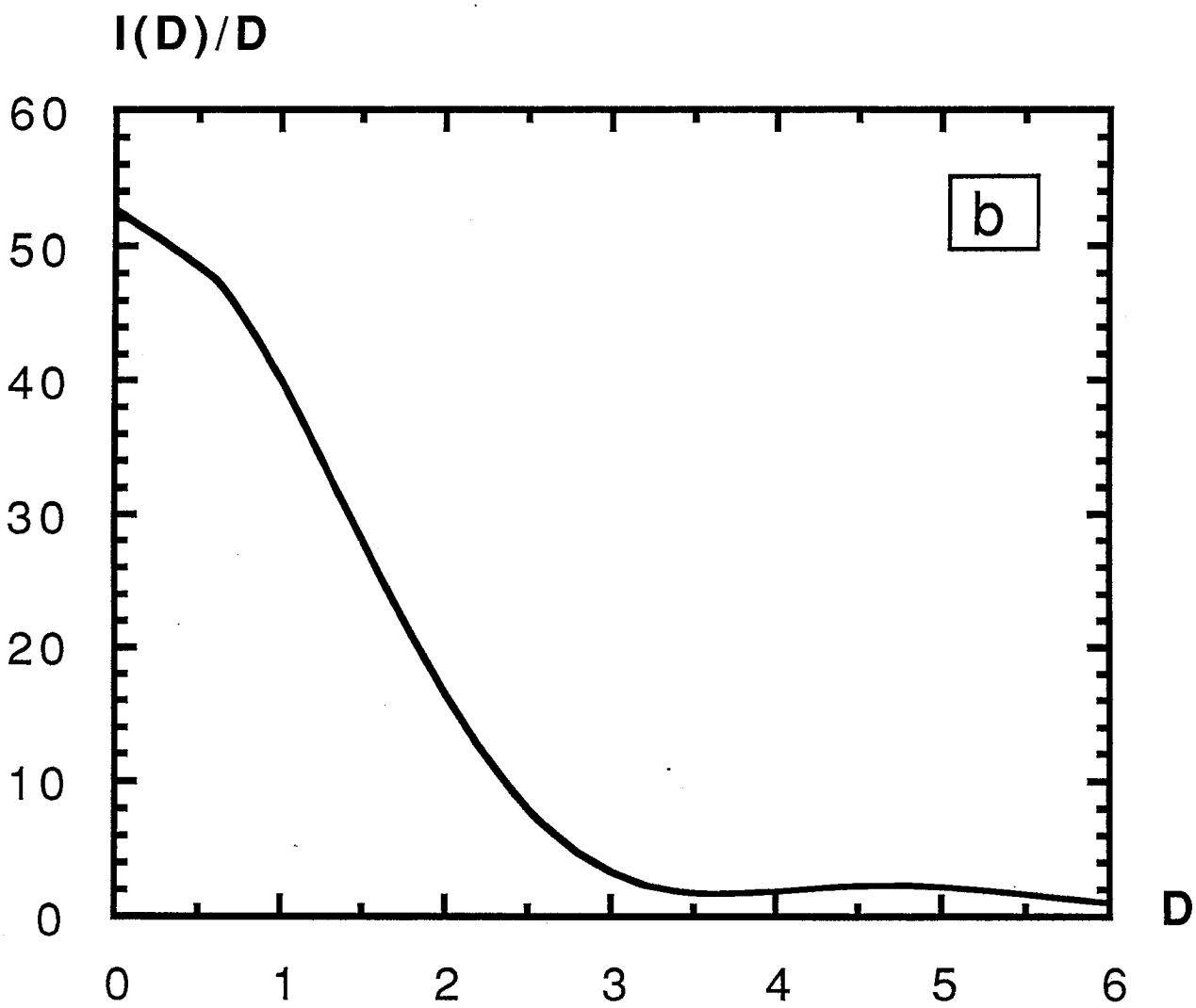

Fig. 1b